

# In Situ TEM Observation of Crystallization of Amorphous Ordered Mesoporous Nb–Ta and Mg–Ta Mixed Oxides

Daling Lu,<sup>†</sup> Tokumitsu Katou,<sup>‡</sup> Miwa Uchida,<sup>‡</sup> Junko N. Kondo,<sup>‡</sup> and Kazunari Domen<sup>\*,†,§</sup>

Core Research for Evolutional Science and Technology Program, Japan Science and Technology, 2-1-13, Higashiueno, Taito-ku, Tokyo, 110-0015 Japan, Chemical Resources Laboratory, Tokyo Institute of Technology, 4259 Nagatsuta, Midori-ku, Yokohama, 226-8503 Japan, and School of Engineering, The University of Tokyo, 7-3-1, Hongo, Bunkyo-ku, Tokyo, 113-8654, Japan

Received August 13, 2004. Revised Manuscript Received November 4, 2004

The crystallization of ordered mesoporous Nb–Ta and Mg–Ta mixed oxides in a vacuum is observed in situ by transmission electron microscopy (TEM). Both metal oxides become polycrystalline upon heating, yet retain the pore size and ordered structure of the amorphous precursors. The crystalline structure and meso-structure of the materials obtained by crystallization in a vacuum differ from those produced by crystallization in air, suggesting the possible role of atmospheric oxygen in the crystallization process.

## Introduction

Since the first report of synthesis of mesoporous silica,<sup>1</sup> there have been many studies on the preparation of various silica-based and metal mesoporous oxides.<sup>2–7</sup> Until recently, the processes used to synthesize mesoporous metal oxides afforded amorphous wall structures. Achieving a crystalline pore-wall structure has been an important issue in attempts to extend the applications of mesoporous materials to fields such as sensors, optical devices, and electrode materials. However, the ordered mesoporous structures are easily destroyed when the amorphous mesoporous materials are crystallized at high temperatures.

Elder et al. calcined an as-synthesized mesoporous Zr–Ti mixed oxide at 450 °C in air to remove the surfactant added in the synthesis process and found that 2.5-nm TiO<sub>2</sub> anatase crystallites appeared in the amorphous zirconia phase.<sup>8</sup> Grosso et al. prepared TiO<sub>2</sub> anatase thin films at 700 °C in air in a short heating process,<sup>9</sup> and the resultant films were found to be composed of crystalline anatase nanoparticles in a well-organized mesoporous network. However, after treatment at 730 °C for 20 min, the anatase aggregated

into particles of larger than 20 nm and the meso-organization was lost. Yang et al. prepared highly ordered single-crystalline In<sub>2</sub>O<sub>3</sub> nanowire arrays with hexagonal and cubic mesostructures,<sup>10</sup> and also successfully synthesized ordered crystallized metal oxide nanoarrays by replication using microwave-digested mesoporous silica.<sup>11</sup> Li et al. designed a “nanocrystal glass” configuration in TO<sub>2</sub>–P<sub>2</sub>O<sub>5</sub>–M<sub>x</sub>O<sub>y</sub> systems (M = metal ion), utilizing the glass phase like a “glue” between nanocrystals as building blocks for the preparation of ordered mesopores.<sup>12</sup>

Although mesoporous metal oxides consisting of crystalline nanoparticles have been realized, it remains difficult to obtain a crystalline metal oxide while retaining the original mesoporous structure of the precursor because the meso-structure easily collapses during the crystallization procedure. Lee et al. synthesized a crystalline Nb–Ta mixed oxide with a wormhole-like mesoporous structure using a two-step calcination process in air and observed that the mesopores of the crystallized material became larger than those in the amorphous precursor.<sup>13–15</sup> This increase in pore size during crystallization was explained as due to poor thermal stability, resulting in the destruction of mesoporous structures. Katou et al. used an “embedding” method to prepare a crystalline mesoporous material. They synthesized a two-dimensional hexagonally ordered mesoporous Nb–Ta mixed oxide<sup>16</sup> and filled the pores with carbon material prior to crystallization in an inert atmosphere.<sup>17,18</sup> The carbon material in the crystallized oxide was later removed by calcination in air to

\* Corresponding author. E-mail: domen@chemsys.t.u-tokyo.ac.jp.

<sup>†</sup> Japan Science and Technology.

<sup>‡</sup> Tokyo Institute of Technology.

<sup>§</sup> The University of Tokyo.

- (1) Kresge, C. T.; Leonowicz, M. E.; Roth, W. J.; Vartuli, J. C.; Beck, J. S. *Nature* **1992**, *359*, 710.
- (2) Hou, Q.; Margolese, D. I.; Ciesla, U.; Demuth, D. G.; Feng, P.; Gier, T. E.; Sieger, P.; Firouzi, A.; Chmelka, B. F.; Schüth, F.; Stucky, G. D. *Chem. Mater.* **1994**, *6*, 1176.
- (3) Ying, J. Y.; Mehnert, C. P.; Wong, M. S. *Angew. Chem., Int. Ed.* **1999**, *38*, 56.
- (4) Yang, P.; Zhao, D.; Margolese, D. I.; Chmelka, B. F.; Stucky, G. D. *Chem. Mater.* **1999**, *11*, 2813.
- (5) Ogawa, M. *Curr. Top. Colloid Interface Sci.* **2001**, *4*, 209.
- (6) Inagaki, S.; Guan, S.; Ohsuna, T.; Terasaki, O. *Nature* **2002**, *416*, 304.
- (7) Davis, M. E. *Nature* **2002**, *417*, 813.
- (8) Elder, S. H.; Gao, Y.; Li, X.; Liu, J.; McCready, D. E.; Windisch, C. F., Jr. *Chem. Mater.* **1998**, *10*, 3140.
- (9) Grosso, G.; Soler-Illia, G. J. de A. A.; Crepaldi, D. L.; Cagnol, F.; Sinturel, C.; Bourgeois, A.; Brunet-Bruneau, A.; Amenitsch, H.; Albouy, P. A.; Sanchez, C. *Chem. Mater.* **2003**, *15*, 4562.

- (10) Yang, H.; Shi, Q.; Tian, B.; Lu, Q.; Gao, F.; Xie, S.; Fan, J.; Yu, C.; Tu, B.; Zhao, D. *J. Am. Chem. Soc.* **2003**, *125*, 4724.
- (11) Tian, B.; Liu, X.; Yang, H.; Xie, S.; Yu, C.; Tu, B.; Zhao, D.; *Adv. Mater.* **2003**, *15*, 1370.
- (12) Li, D.; Zhou, H.; Honma, I. *Nat. Mater.* **2004**, *3*, 65.
- (13) Lee, B.; Lu, D.; Kondo, J. N.; Domen, K. *Chem. Commun.* **2001**, 2118.
- (14) Lee, B.; Yamashita, T.; Lu, D.; Kondo, J. N.; Domen, K. *Chem. Mater.* **2002**, *14*, 867.
- (15) Kondo, J. N.; Yamashita, T.; Katou, T.; Lee, B.; Lu, D.; Hara, M.; Domen, K. *Stud. Surf. Sci. Catal.* **2002**, *141*, 265.
- (16) Katou, T.; Lu, D.; Kondo, J. N.; Domen, K. *J. Mater. Chem.* **2002**, *12*, 1480.

**Table 1. Textural Properties of Nb–Ta and Mg–Ta Mixed Oxides**

	<i>d</i> (100) value (nm)	mean pore size (nm)	pore volume (mL·g <sup>-1</sup> )	BET surface area (m <sup>2</sup> ·g <sup>-1</sup> )	wall thickness <sup>a</sup> (nm)
Nb–Ta oxide	7.4	5.6	0.34	184	2.9
Mg–Ta oxide	6.7	5.0	0.28	123	2.8

<sup>a</sup> Wall thickness was estimated from *d*(100) and the mean pore size in the two-dimensional hexagonal mesoporous structure.

afford a crystalline Nb–Ta metal oxide with a mesoporous structure. Tian et al. employed a “replica” method to prepare a crystalline metal oxide with a mesoporous structure. They added hydrated metal nitrates to ordered mesoporous silica as a template.<sup>19</sup> After calcination in air to crystallize the metal oxides, the silica was dissolved with NaOH to yield crystalline metal oxides with intact meso-structures.

Although the destruction of the mesoporous structure during crystallization has been explained as simply being due to poor thermal stability of the mesoporous materials, there have been no detailed explanations of the mechanism of destruction or enlargement of mesopores in the crystallization procedure. In this paper, in situ transmission electron microscopy (TEM) observations of the crystallization of mesoporous Nb–Ta and Mg–Ta mixed oxides by heating in a vacuum are made to clarify what happens to these materials during crystallization.

### Experimental Section

The synthesis of Nb–Ta and Mg–Ta mixed oxides has been described in detail elsewhere.<sup>16,20</sup> Under continuous stirring for 10 min, 1 g of the triblock copolymer HO(CH<sub>2</sub>CH<sub>2</sub>O)<sub>20</sub>(CH<sub>2</sub>CH(OH)CH<sub>2</sub>O)<sub>70</sub>(CH<sub>2</sub>CH<sub>2</sub>O)<sub>20</sub>H (EO<sub>20</sub>PO<sub>70</sub>EO<sub>20</sub>; Pluronic P-123, BASF) was dissolved in 10 g of dehydrated ethanol (99.5%, Kanto Chemical Co.) as a structure-directing surfactant. In the case of Nb–Ta, 0.0055 mol of a mixture of NbCl<sub>5</sub> (99.9%) and TaCl<sub>5</sub> (99.99%) (mole ratio of Nb/Ta = 1) was added to this solution under vigorous stirring for 20 min, followed by the addition of 0.018 mol of water with further stirring for 10 min. Adding a trace amount of water has been found to improve the mesoporous structure.<sup>16</sup> In the case of Mg–Ta, 0.01 mol of a mixture of TaCl<sub>5</sub> and MgCl<sub>2</sub> (99.99%) (mole ratio of Ta/Mg = 2) was added under stirring for 30 min. All metal chlorides were purchased from Rare Metallic Co. The resulting sol was placed in a Petri dish for gelation at 40 °C in air for 3 days (Nb–Ta) or 7–10 days (Mg–Ta). The aged gel was then calcined in air at 450 °C for 5 h (Nb–Ta) or 500 °C for 30 h (Mg–Ta) to remove the surfactant.

X-ray diffraction (XRD) patterns were obtained on a Rigaku RINT 2100 diffractometer with Cu Kα radiation. Crystallization temperatures of the mixed oxides were measured by differential thermal analysis (DTA) and thermogravimetry (TG) using a Shimadzu DTG-50 in air at a heating rate of 10 °C·min<sup>-1</sup>. The surface areas of the two oxides were calculated from nitrogen gas adsorption–desorption isotherms obtained using Coulter Omnisorp

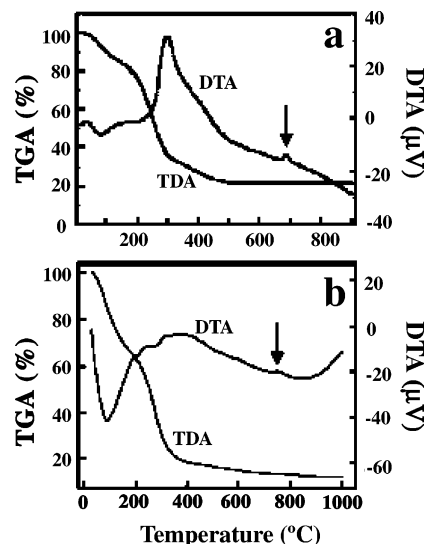


**Figure 1.** TG/DTA analysis of template-containing (a) Nb–Ta oxide and (b) Mg–Ta oxide. Peaks indicated by arrows represent crystallization temperatures.

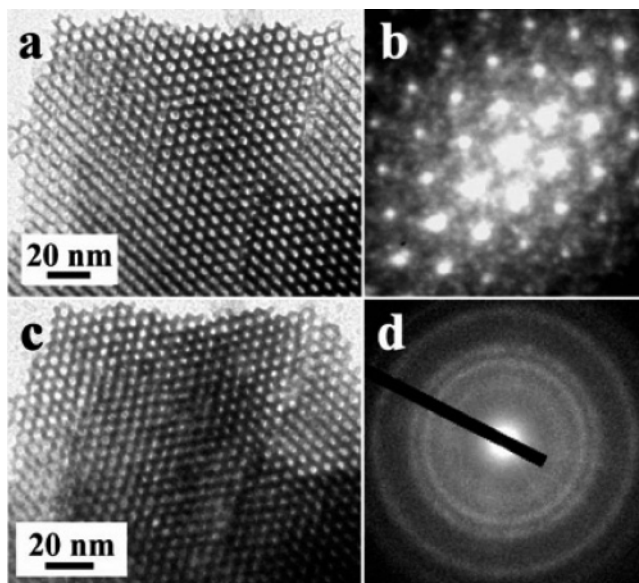


**Figure 2.** (a) TEM image of a mesoporous Nb–Ta mixed oxide particle at room temperature and (b) the corresponding SAED pattern (*L* = 200 cm). (c) TEM image of the same particle after heating to 550 °C, and (d) corresponding SAED pattern (*L* = 100 cm).

100CX and SA-31000 systems. Pore-size distributions were determined by Barrett–Joyner–Halenda (BJH) analysis, and pore volumes were calculated based on the pore-size distribution between 2 and 50 nm.

TEM samples of the Nb–Ta and Mg–Ta mixed oxide were prepared by ultrasonication in 2-propanol and subsequent suspension on carbon-coated Mo grids. TEM observations were carried out using a high-resolution field-emission TEM (JEM-2010F, JEOL) operating at 200 keV with a specimen-heating holder capable of heating to 800 °C. As the Nb–Ta (or Mg–Ta) mixed oxide samples had already been calcined at 450–500 °C for removal of the surfactant, the TEM samples were heated at 5 °C·min<sup>-1</sup> from 450/500 to 800 °C. Heating was paused every 50 °C for in situ TEM observation, allowing 10 min at each temperature for stabilization.

### Results

The amorphous precursors, mesoporous Nb–Ta and Mg–Ta mixed oxides, have a highly ordered, two-dimensional

- (17) Katou, T.; Lee, B.; Lu, D.; Kondo, J. N.; Hara, M.; Domen, K. *Stud. Surf. Sci. Catal.* **2002**, *141*, 251.
- (18) Katou, T.; Lee, B.; Lu, D.; Kondo, J. N.; Hara, M.; Domen, K. *Angew. Chem., Int. Ed.* **2003**, *42*, 2382.
- (19) Tian, B.; Liu, X.; Solovyov, L. A.; Liu, Z.; Yang, H.; Zhang, Z.; Xie, S.; Zhang, F.; Tu, B.; Yu, C.; Terasaki, O.; Zhao, D. *J. Am. Chem. Soc.* **2004**, *126*, 865.
- (20) Uchida, M.; Kondo, J. N.; Lu, D.; Domen, K. *Chem. Lett.* **2002**, *5*, 498.

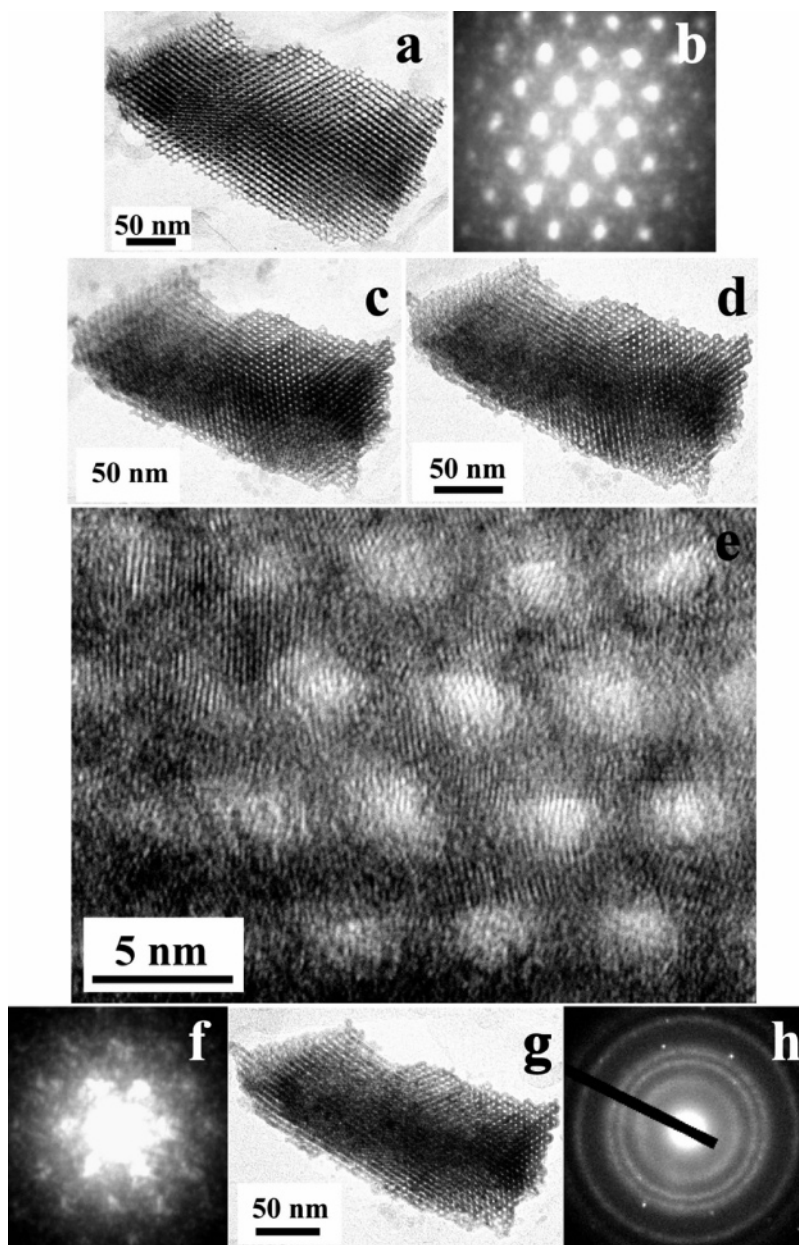


**Figure 3.** (a) TEM image of a mesoporous Nb-Ta mixed oxide particle at room temperature, and (b) corresponding SAED pattern ( $L = 200$  cm). (c) TEM image of the same particle at 650 °C, and (d) 750 °C. (e) High-magnification TEM image of a part of (d). (f) The corresponding SAED pattern ( $L = 200$  cm) of the particle shown in Figure 3g, describing the existence of hexagonally ordered mesoporous structure. (g) TEM image of the same particle at 800 °C. (h) The corresponding SAED pattern ( $L = 100$  cm) of the particle shown in Figure 3g, representing that this mesoporous particle has been crystallized as a polycrystal.

hexagonal structure, as reported previously.<sup>16,20</sup> The textural properties of the ordered mesoporous mixed oxides are summarized in Table 1.

DTA and TG measurements of the template-containing Nb-Ta and Mg-Ta mixed oxides are shown in Figure 1. The TG curves indicate that the template in both mixed oxides was completely eliminated at 400–500 °C. An exothermic peak in the DTA curve (indicated by an arrow) emerged without any weight loss in the high-temperature region as shown in Figure 1a and b, suggesting crystallization of the Nb-Ta and Mg-Ta mixed oxides. The crystallization temperature was found to be about 690 °C for Nb-Ta, and 750 °C for Mg-Ta oxides.

Figure 2a is a TEM image of a Nb-Ta mixed oxide particle observed at room temperature, showing an ordered

mesoporous structure in the particle. The corresponding selected-area electron diffraction (SAED) pattern of this particle (Figure 2b) evidences the hexagonally ordered structure in the particle, and the direction parallel to the straight channels in the two-dimensional mesoporous structure is slightly tilted toward the incident electron beam. From the DTA results for the Nb-Ta oxide (Figure 1a), the amorphous mesoporous Nb-Ta mixed oxide appears to begin crystallizing in air at about 690 °C. However, in the present in situ observations, the Nb-Ta oxide began to crystallize at 550 °C. Figure 2c shows a TEM image of the Nb-Ta particle in Figure 2a, taken after the sample was heated to 550 °C. The directions of the mesoporous channels in the particle at 500 °C deviate slightly from the original position at room temperature, and the ordered mesoporous



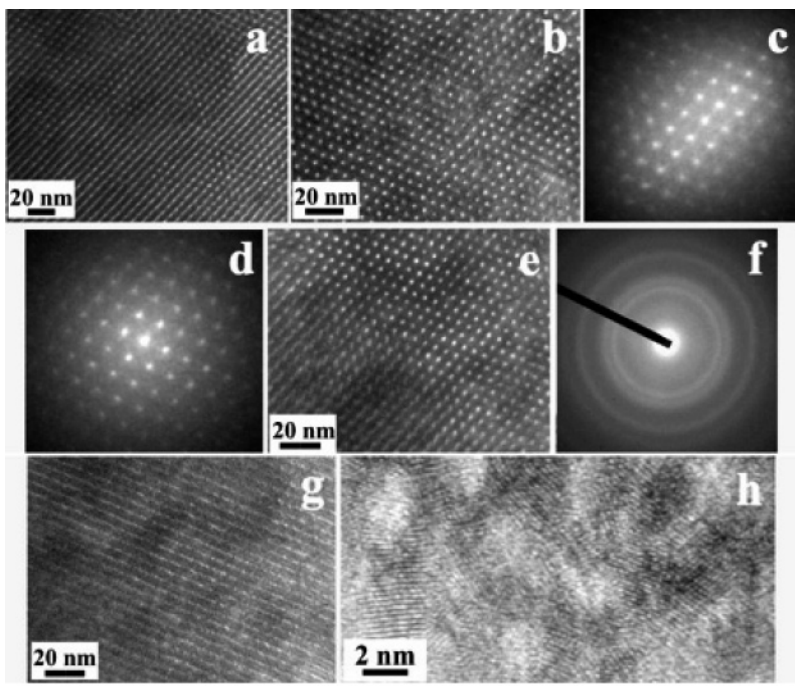


**Figure 4.** (a) TEM image of part of a Mg-Ta mixed oxide particle at room temperature. (b) TEM image of the same particle at 650 °C, and (c) the corresponding SAED pattern ( $L = 200$  cm). (d) The corresponding SAED pattern ( $L = 200$  cm) of the particle shown in Figure 4e, describing the existence of hexagonally ordered mesoporous structure. (e) TEM image of the same particle at 750 °C. (f) The corresponding SAED pattern ( $L = 100$  cm) of the particle shown in Figure 4e, representing that this mesoporous particle has been crystallized as a polycrystal. (g) TEM image of the same particle at 800 °C and (h) high-magnification image of Figure 4g.

structure of this particle becomes indistinct at 550 °C. The corresponding SAED pattern (Figure 2d) of the particle heated at 550 °C is a weak ring pattern, indicating that the particle was already crystallized to a low degree at this temperature and that the crystallized particles are polycrystalline.

The face distances of crystals can be calculated from the SAED pattern using the following equation:

$$dR = L\lambda \quad (1)$$

where  $d$  is a face distance in the sample,  $R$  is the distance between the transmission spot and a diffraction spot,  $L$  is the SAED camera length, and  $\lambda$  is the wavelength of the incident electron beam. If  $L$  and  $\lambda$  are constants,  $R$  becomes smaller as  $d$  becomes larger. Generally, the face distances of various inorganic materials are on the order of angstroms. However, the face distances of mesoporous structures are usually in the region of nanometers. If the same camera length is used to take SAED images of the mesoporous structures and crystals,  $R$  would be too large or too small to be measured. For clear observation of the diffraction patterns of both mesoporous structures and crystals, a camera length of 200 cm was employed for meso-structure observation (Figure 2b), and  $L = 100$  cm was used to observe crystals (Figure 2d). The SAED pattern in Figure 2b is thus magnified by several times compared to Figure 2d for clarity, but it should be noted that  $R$  in the two figures is not comparable.

Figure 3 shows a series of in situ TEM images of another Nb-Ta mixed oxide particle taken during a heating procedure. The TEM image (Figure 3a) and the corresponding SAED pattern (Figure 3b,  $L = 200$  cm) at room temperature verify the presence of a hexagonally ordered mesoporous structure in the particle. Figure 3c and 3d also demonstrate

the mesoporous structure in the particles upon heating to 650 and 750 °C, respectively. As the particle was very thin, it bent slightly during the heating procedure, resulting in a slightly narrower profile in projection at higher temperatures. Some of the channels that were initially parallel with the incident electron beam also deviated from the direction of the electron beam at higher temperatures due to this bending, causing the ordered mesoporous structure to be less clear in the TEM images. A high-magnification image (Figure 3e) of the particle heated at 750 °C reveals clear lattice fringes. As the straight channels of the mesopores deviated from the incident electron beam, the lattice image of the crystallized wall structure overlaps in the brighter round areas, representing the pore-openings of tilted straight channels of the mesopores.

The mesoporous structure of the particle could still be observed even when the particle was heated to 800 °C (Figure 3g). The corresponding hexagonal SAED pattern ( $L = 200$  cm) of the heated particle (Figure 3f) also indicates the presence of an ordered mesoporous structure after heating to 800 °C. The SAED pattern in Figure 3f is not as clear as that in Figure 3b because the direction of most straight channels in the particle at 800 °C had begun to diverge from the direction of the incident electron beam. Figure 3h shows the corresponding SAED ring pattern ( $L = 100$  cm) for the whole particle shown in Figure 3g. The figure shows that the particle was polycrystalline, not single-crystalline as found previously.<sup>14</sup> The higher intensity of the SAED pattern in Figure 3h compared to that in Figure 2d reflects the higher crystallinity of the former. Comparing Figure 3a, c, d, and g, the original mesoporous structure and pore-size of the particle appear to have been maintained during heating to 800 °C.

Crystallization of the mesoporous metal oxide in a vacuum without destroying the meso-structure was also successful for the Mg–Ta mixed oxide. Figure 4 shows a series of in situ images of a mesoporous Mg–Ta oxide particle taken during the heating process. The TEM image taken at room temperature (Figure 4a) shows that the direction of the majority of mesoporous channels had diverged slightly from the direction of the incident electron beam. After heating to 650 °C, the mesopores became oriented almost parallel to the incident electron beam (Figure 4b). The corresponding SAED pattern in Figure 4c ( $L = 200$  cm) shows the presence of a hexagonal ordered mesoporous structure. Increasing the temperature to 750 °C caused about one-quarter of the mesoporous structure to become indistinct due to tilt of the mesoporous channels (Figure 4e). However, the corresponding SAED pattern (Figure 4d,  $L = 200$  cm) indicates that the particle still retains a hexagonally ordered mesoporous structure. Figure 4f shows another SAED ring pattern ( $L = 100$  cm) of the particle in Figure 4e. The ring pattern indicates that crystallization of this Mg–Ta oxide particle started at 750 °C, consistent with the DTA results, which gave a crystallization temperature of about 750 °C. Upon heating to 800 °C, the direction of most channels in the Mg–Ta particle deviated by several degrees from alignment with the incident electron beam, making the mesoporous structure difficult to observe (Figure 4g). A high-magnification TEM image of the Mg–Ta oxide particle heated to 800 °C (Figure 4h) exhibits bright areas corresponding to mesopores, and crystals of several nanometers in size forming the walls. Comparing Figure 4a, b, e, and g, the mesoporous structure appears to have remained intact during heating to 800 °C, and the mesopores did not become larger. These characteristics are similar to those for the Nb–Ta mixed oxide mentioned above.

### Discussion

Whereas the pore size of the Nb–Ta mixed oxide with wormhole-like mesoporous structure expanded from 4 to 10 nm upon crystallization in air at 650 °C,<sup>14</sup> no apparent change in the pore size of the particles was observed upon crystallization in a vacuum at 800 °C in the present experiment. Furthermore, crystallization in air produced a single-crystal wall structure, whereas crystallization in a vacuum produced a polycrystalline structure. At present, there is no clear explanation for this difference in crystallization behavior. In air, the particles crystallize in the presence of oxygen. Thus, the different crystallization processes may be tentatively attributed to the presence or absence of oxygen.

In the catalytic oxidation of propylene, once atmospheric oxygen adsorbs onto the surface of the bismuth molybdate catalyst, it rapidly diffuses into the catalyst material to equilibrate with the oxygen ions in the bulk.<sup>21</sup> Moro-Oka and Ueda systematically investigated various reactions on bismuth molybdate catalyst and found that  $^{18}\text{O}_2$  in the atmosphere exchanges with  $^{16}\text{O}$  in the catalyst bulk.<sup>22</sup> On the surface of several crystalline oxides, atmospheric  $^{18}\text{O}_2$

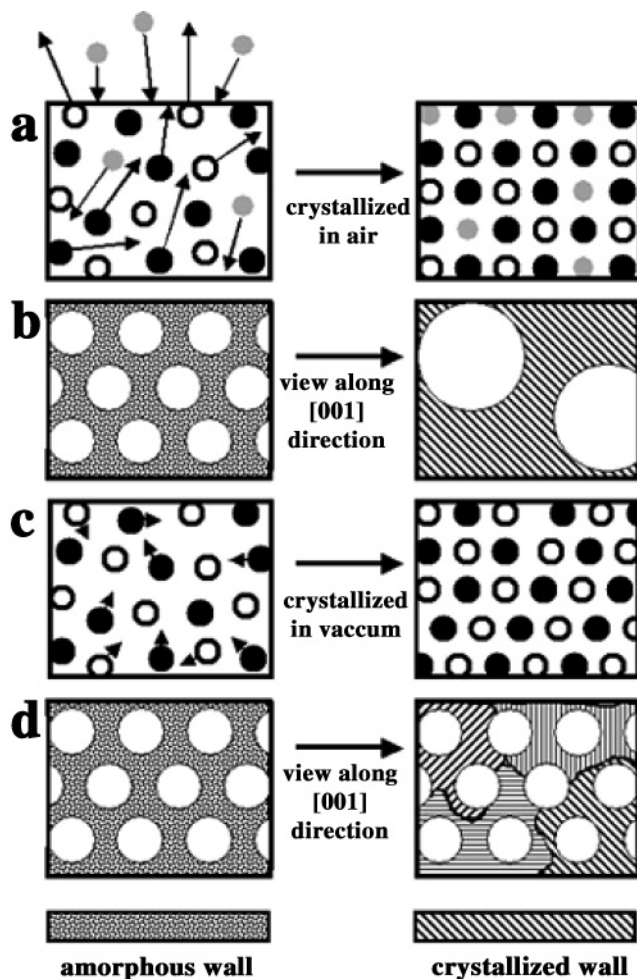


**Figure 5.** Schematic representation of crystallization process for mesoporous metal oxides in air and a vacuum. Crystallization process in air, showing (a) exchange of oxygen in air with oxygen in metal oxide, and (b) view along the [001] direction of the resultant mesoporous material. Crystallization process in a vacuum, showing (c) suppressed oxygen exchange, and (d) view along the [001] direction of the resultant mesoporous material. Grey circles indicate oxygen in air, open circles indicate oxygen in the bulk, black circles indicate metal atoms in the bulk. The length of arrows expresses the range of movement of atoms.

has also been shown to readily exchange with lattice  $^{16}\text{O}$  above a certain temperature<sup>23</sup> by interaction with  $^{18}\text{O}_2$  species adsorbed on metal atoms on the oxide surface. This process also involves the diffusion of bulk oxygen species to the surface to exchange with adsorbed  $^{18}\text{O}_2$  species as a result of the thermal weakening of the metal–oxygen bonds and corresponding increase in oxygen mobility.

On the basis of these previous findings and the results of the present experiments, the dissimilar mechanisms of crystallization in air and in a vacuum may be explained as follows. When the amorphous mesoporous Nb–Ta mixed oxide is heated in air, the metal–oxygen bonds become weakened, and surface oxygen species exchange with air-derived oxygen species adsorbed to the metal oxide surface. These two processes induce the diffusion of bulk oxygen species to the surface and the long-range movement of Nb and Ta metal atoms to achieve an optimum rearrangement. During this crystallization procedure, mass transfer occurs over a large region, with the originally small mesopores

(21) Keulks, G. W. *J. Catal.* **1970**, *19*, 232.

(22) Moro-Oka, Y.; Ueda, W. *Adv. Catal.* **1994**, *40*, 233.

(23) Martin, D.; Duprez, D. *J. Phys. Chem.* **1996**, *100*, 9429.

merging into larger mesopores to minimize the total surface energy. This long-range movement of Nb and Ta allows for the formation of single-crystalline particles of hundreds of nanometers in diameter through minimization of lattice distortion energy during phase transference from amorphous to crystalline, as observed previously.<sup>14</sup>

A schematic representation of this process is shown in Figure 5. When the amorphous mesoporous metal oxide is crystallized in air, the oxygen in air exchanges with the oxygen in the oxide, promoting the long-range mobility of metal atoms (Figure 5a). Because of this long-range mass transfer, the originally small mesopores merge into larger pores as the single-crystalline structure is formed (Figure 5b). On the other hand, when the amorphous mesoporous Nb–Ta mixed oxide is heated in a vacuum, oxygen exchange at the surface would be suppressed, preventing the long-range diffusion of bulk oxygen and limiting the range of mobility of Nb and Ta atoms. Thus, neither mass transfer nor metal atom movement occurs over a wide range, resulting in the localized formation of crystals in a polycrystalline structure (Figure 5c and d). This limited mobility and transport would also preserve the original pore size, as demonstrated in the present in situ observations. Viewing the mesoporous structure along the [001] direction, parallel to the direction of straight channels in the two-dimensional mesoporous material, the pore size will remain unchanged upon crystallization. The same explanation is considered to be valid for the Mg–Ta mixed oxide.

In the present experiments, the ordered mesoporous structure of some Nb–Ta and Mg–Ta mixed oxide particles

appeared to have been damaged or could not be observed after heating. As the walls of the mesoporous mixed oxides are relatively thin (2–3 nm), damage to the wall structure may occur quite easily during the heating procedure. Similarly, the thin wall structures are susceptible to bending upon heating, causing the orientation of the mesopores to shift from a uniform alignment, thus rendering the mesopores unobservable by TEM.

### Conclusion

In this study, the crystallization of amorphous ordered mesoporous Nb–Ta and Mg–Ta mixed oxides was investigated by in situ TEM observation. It was found that both materials form polycrystalline products with mesopore sizes equivalent to those of the precursors upon heating to 800 °C. It is suggested that, due to the lack of oxygen during crystallization in a vacuum, the range of mobility of metal atoms is restricted, and mass transfer is suppressed, resulting in highly localized crystallization and the formation of a polycrystalline structure with the original pore size. The present in situ study has revealed that it is possible to obtain crystallized metal oxides with a predictable, ordered mesoporous structure under certain conditions.

**Acknowledgment.** This work was supported under the Core Research for Evolutional Science and Technology (CREST) program of the Japan Science and Technology (JST) Corporation and the 21st Century Center of Excellence (COE) program of the Ministry of Education, Science, Sports and Culture of Japan.

CM048660G